Journal of Geophysical Research: Biogeosciences

RESEARCH ARTICLE
10.1029/2018JG004436

Control of Nitrogen Exports From River Basins to the Coastal Ocean: Evaluation of Basin Management Strategies for Reducing Coastal Hypoxia

M. Lee[1], C. Jung[2], E. Shevliakova[3], S. Malyshev[3], H. Han[4], S. Kim[2], K. Kim[5], and P. R. Jaffé[6]

[1]Program in Atmospheric and Oceanic Sciences, Princeton University, Princeton, NJ, USA, [2]Department of Civil and Environmental Systems Engineering, Konkuk University, Seoul, South Korea, [3]NOAA/Geophysical Fluid Dynamics Laboratory, Princeton, NJ, USA, [4]Division of Water Environment, Environment Institute, Sejong, South Korea, [5]Water Environment Research Department, Water Quality Control Center, Institute of Environmental Research, Incheon, South Korea, [6]Department of Civil and Environmental Engineering, Engineering Quadrangle, Princeton University, Princeton, NJ, USA

Abstract The spread of coastal hypoxia is a pressing global problem, largely caused by substantial nitrogen (N) exports from river basins to the coastal ocean. Most previous process-based modeling studies for investigating basin management strategies to reduce river N exports focused on the impacts of different farming practices or land use, used watershed models that simplified many mechanisms that critically affect the state of N storage in land, were limited mainly to fairly small basins, and did not span multiple climate regimes. Here we use a process-based land-river model to simulate historical (1999–2010) river flows and nitrate-N exports throughout the entire drainage network of South Korea (100,210 km^2), which encompasses varying climate, land use, and hydrogeological characteristics. Based on projections by using multiple scenarios of N input reductions and climates, we explore the impacts of various ecosystem factors (i.e., N storage in basins, climate and its variability, anthropogenic N inputs, and basin location) on river nitrate-N exports. Our findings have fundamental implications for reducing coastal hypoxia: (1) a small reduction of N inputs in basins, including intensively utilized human land use, can have a greater improvement on water quality; (2) heightening climate variability may not increase long-term mean river N exports yet can significantly mask N input reduction effects by producing N export extremes associated with recurring coastal hypoxia; and (3) N exports to the coastal ocean can be most efficiently reduced by decreasing N inputs in subbasins, which are receiving high anthropogenic N inputs and are close to the coast.

Key Points:
- A small reduction of nitrogen inputs in basins, with intensive human land use, can have a greater improvement on water quality
- Climate variability may not increase long-term mean river nitrogen exports yet can produce export extremes related to coastal hypoxia
- Coastal nitrogen exports can be efficiently reduced by targeting basins that are receiving high nitrogen inputs and are close to the coast

Supporting Information:
- Supporting Information S1
- Data Set S1
- Data Set S2

Correspondence to:
M. Lee,
minjinl@princeton.edu

Citation:
Lee, M., Jung, C., Shevliakova, E., Malyshev, S., Han, H., Kim, S., et al. (2018). Control of nitrogen exports from river basins to the coastal ocean: Evaluation of basin management strategies for reducing coastal hypoxia. *Journal of Geophysical Research: Biogeosciences*, *123*, 3111–3123. https://doi.org/10.1029/2018JG004436

Received 6 FEB 2018
Accepted 10 SEP 2018
Accepted article online 17 SEP 2018
Published online 4 OCT 2018

1. Introduction

The spread of coastal hypoxia (defined as dissolved oxygen levels ≤2 ml/L) is a pressing global problem (Diaz & Rosenberg, 2008), causing severe socioeconomic consequences, such as habitat-quality degradation, food-web collapse, and fish kills in marine ecosystems (Breitburg, 2002; Diaz & Rosenberg, 1995; Paerl et al., 1998). Nitrogen (N) enrichment in coastal waters often leads to excessive growth of algae, which, in turn, die, sink to the ocean floor, and stimulate decay processes, consuming dissolved oxygen from bottom waters. Accordingly, recognized as one of the major culprits for the spread of coastal hypoxia worldwide are dramatically increased production of bioavailable N in basins over the last century, mainly by human activities of fossil fuel combustion and crop cultivation with synthetic fertilizer applications (Galloway et al., 2004, 2008; Smil, 1999), and its substantial exports by large rivers to the coastal ocean (Howarth & Marino, 2006; Howarth et al., 2002). A number of previous observational studies found significant relationships between N exports from large rivers and coastal hypoxia (e.g., Susquehanna River/Chesapeake Bay, Hagy et al., 2004; Kemp et al., 2005; Murphy et al., 2011; and Mississippi River/Gulf of Mexico, Rabalais et al., 1999, 2007, 2002).

Previous empirical studies showed that the mechanisms that control N exports from river basins to the coastal ocean are complex and nonlinear, as they are influenced by multiple region-specific ecosystem factors, such as long-term mean climate (Howarth et al., 2006), short-term climate variability (Kaushal et al., 2008), changes in land use or anthropogenic N inputs like fertilizer applications (Johnes, 1996; Mulholland et al., 2008), and river channel size or depth (Alexander et al., 2000; Peterson et al., 2001). Process-based modeling approaches can provide a mean of exploring the role of such ecosystem factors in river N exports for regions influenced by various climate, anthropogenic N inputs, and hydrogeological characteristics.

Table 1
Descriptions of 11 Basins Across South Korea

Site	River basin	Flow site	Water quality site	N input rate (kg·km^{-2}·year^{-1})	Precipitation (mm/year^{-1})
A	Han	Hangangdaegyo	Yeongdeungpo	3,006	1,475
B	Han	Yeongwol	Yeongwol1	2,388	1,364
C	Han	Yeongwol1	Pyeongchanggang3	2,435	1,364
D	Nakdong	Samrangjin	Samrangjin	3,097	1,444
E	Nakdong	Andong Dam	Dosan	2,055	1,209
F	Nakdong	Hapcheon Dam	Hwanggang1	3,403	1,679
G	Geum	Gongju	Gongju1	3,456	1,536
H	Seomjin	Gurye2	Gurye	3,742	1,759
I	Seomjin	Seomjingang Dam	Unam	3,301	1,730
J	Yeongsan	Yeongsanpo	Yeongsanpo	5,488	1,626
K	Yeongsan	Mareuk	Gwangju2	5,374	1,524
Site	Basin area (km^2)	Urban area km^2 (%)	Agricultural area km^2 (%)	Forested area km^2 (%)	Other area km^2 (%)
A	25,232	1,187 (5)	3,309 (13)	16,737 (66)	3,999 (16)
B	2,448	31 (1)	258 (11)	2,106 (86)	53 (2)
C	1,773	27 (2)	272 (15)	1,433 (81)	42 (2)
D	22,892	946 (4)	5,201 (23)	15,427 (67)	1,318 (6)
E	1,584	26 (2)	203 (13)	1,340 (85)	16 (1)
F	925	25 (3)	200 (22)	659 (71)	41 (4)
G	7,150	394 (6)	1,828 (26)	4,746 (66)	182 (3)
H	3,810	103 (3)	865 (23)	2,520 (66)	322 (9)
I	763	17 (2)	152 (20)	535 (70)	59 (8)
J	2,142	164 (8)	615 (29)	855 (40)	509 (24)
K	684	111 (12)	216 (23)	316 (34)	41 (4)

Note. Basin-wide mean N input rates in 2010, basin-wide mean precipitation from the 2010 forcing data (Sheffield et al., 2006), basin areas, and various land use areas for the 11 Ministry of Land, Infrastructure and Transport flow and 11 National Institute of Environmental Research nutrient monitoring sites in the five river basins.

Nonetheless, particularly for the purpose of investigating basin management strategies, most previous process-based watershed models were applied only for studies of fairly small basins (mostly much less than 20,000 km^2) that do not cover different climate regimes (e.g., Chaplot et al., 2004; Hu et al., 2007; Jha et al., 2007; Krause et al., 2008; Schilling & Wolter, 2009; Wendland et al., 2005). This was because of their focus on the local impacts of different farming practices or land use changes on river N exports. Furthermore, this class of models simplifies and/or neglects many coupled carbon (C) and N dynamics on a decadal-to-century time scale (e.g., land use and land cover changes [LULCC] and associated mechanisms, such as forest clearing for agriculture, wood harvesting, and forest regrowth after harvesting) that critically affect the state of vegetation-soil N storage in land. Under centennial-scale history of increases in atmospheric CO_2 and LULCC, capturing temporal and spatial N storage in land is challenging but also imperative because water N pollution responses to anthropogenic N inputs strongly depend on the state of N storage in land (McLauchlan et al., 2013).

The process-based Geophysical Fluid Dynamic Laboratory LM3-terrestrial and aquatic nitrogen (TAN) model (Lee et al., 2014) addressed the aforementioned limitations of watershed models and captures TAN cycling in response to decadal-to-century changes in mean climate and LULCC as well as short-term (seasonal to multi-year) climate variability and extremes (Lee et al., 2016). A recent process-based watershed modeling study explored the effect of long-term legacy land N storage on river N exports while reducing N inputs (Van Meter et al., 2018), but its exploration was only limited to N storage impacts. To advance basin management strategies, therefore, it is imperative to explore various ecosystem factors (e.g., N storage in basins, climate and its variability, anthropogenic N inputs, and basin location) and how those factors are related to control mechanisms of N exports from river basins to the coastal ocean, by using a comprehensive process-based model like LM3-TAN.

South Korea is a good study site to explore global issues of coastal N pollution, because *red tides* in coastal waters around the Korean Peninsula indicate severe land-derived N pollution, despite enaction of rigorous legislation for country-wide basin management over decades (Organisation for Economic Cooperation and Development [OECD], 1997; OECD, 2006). South Korea is composed of five major river basins (Table 1 and

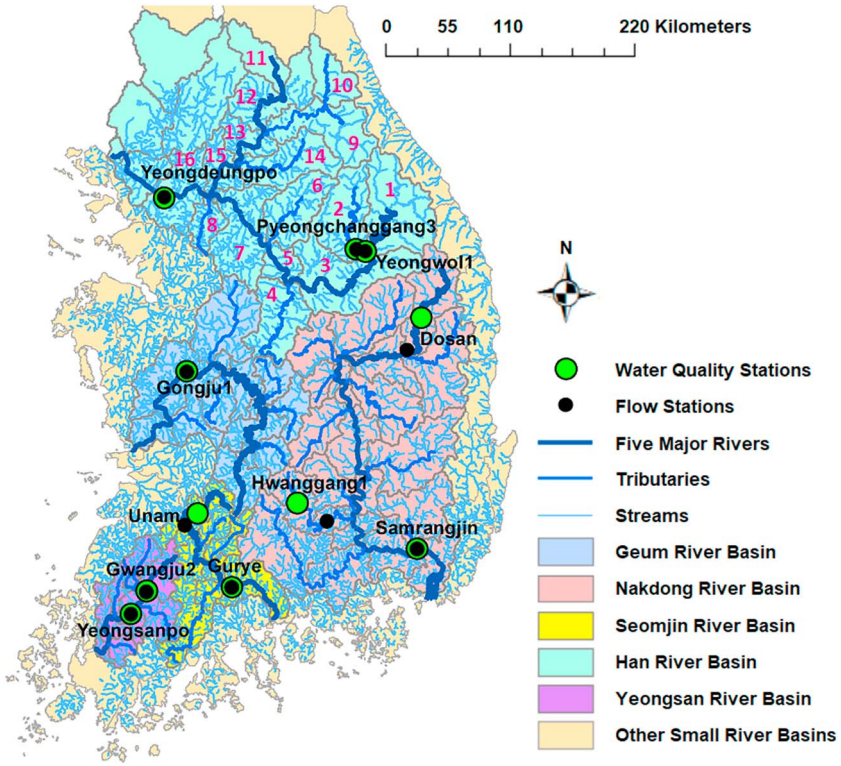

Figure 1. Map of the five river basins in South Korea. Main stems of the five rivers, their major tributaries, and the locations of the 11 Ministry of Land, Infrastructure and Transport flow and 11 National Institute of Environmental Research nutrient monitoring sites. The 16 subbasins in the Yeongdeungpo site basin are marked by numbers from 1 to 16.

Figure 1). The country is influenced by different climates (i.e., humid continental and subtropical) and various land use (i.e., 63.8% forest or other wooded land, 19.0% arable and permanent crop land, 0.5% permanent grass land, and 16.7% other areas for the year 2006; OECD, 2006). Among the OECD countries, South Korea displays one of the highest rates of economic growth and the highest population density (OECD, 1997, 2006). Especially, the largest river in South Korea, Han River, drains an area of 26,219 km^2 and its basin, including the Seoul-Incheon metropolitan area with 25 million residents (about half of the country's population), has experienced one of the rapidest urbanization and increases in the number of vehicles. As a result, the Han River has suffered from severe N-enrichment problems (Chang, 2008), which is of special concern, because this river is the primary water source for drinking, irrigation, and industrial use for about half of the country's population. The river also contributes to eutrophication in the Han River estuary, resulting in undesirable ecological changes in the ecosystem (Hyun et al., 1999).

In this study, we use various scenarios of N input reductions and climates to project river nitrate-N exports throughout the entire drainage network of South Korea (100,210 km^2), which is influenced by diverse climates, land use, and human activities as described above. These projections thus allow analyzing the role of spatially varying ecosystem factors across the country in river nitrate-N exports under countrywide as well as local N input reduction scenarios. Based on the analyses, regions representing high N input reduction efficiency are also identified, with implications for effective basin management strategies. We do these by (1) simulating river nitrate-N exports from 1999 to 2010, (2) evaluating the simulations based on measurement-based estimates, (3) projecting nitrate-N exports from 2011 to 2073, and (4) using the projected results to calculate N input reduction efficiency ratios for different basins and subbasins.

2. Materials and Methods

2.1. Descriptions of Monitoring Sites and Reported Data

Twenty-two monitoring sites were chosen to evaluate the model results for the period 1999–2010 (Figure 1 and Table 1): 11 river flow monitoring sites, operated by the Ministry of Land, Infrastructure and Transport,

Table 2
Descriptions of Six Grouped Subbasins in the Yeongdeungpo Site Basin

Group	Subbasins	Subbasin areas (km^2)	Distance from Yeongdeungpo (m)	N input rates ($kg{\cdot}km^{-2}{\cdot}year^{-1}$)	N inputs (kt/year)
a	1, 2	4,221	204,004	2,543	10.74
b	3, 4	4,098	132,852	2,795	11.46
c	4, 5, 6	3,630	97,310	3,072	11.15
d	7	2,073	61,814	5,497	11.39
e	9, 10, 12	4,371	128,871	2,601	11.37
f	13, 14, 15	3,048	61,814	3,340	10.18

Note. Six grouped subbasin areas, distances from the Yeongdeungpo site to the six grouped subbasins, subbasin-wide mean anthropogenic N input rates ($kg{\cdot}km^{-2}{\cdot}year^{-1}$), and N inputs (kt/year) in 2010 for the six grouped subbasins.

and 11 nutrient monitoring sites, operated by the National Institute of Environmental Research. The Hangangdaegyo/Yeongdeungpo, Samrangjin, Gongju/Gongju1, Gurye2/Gurye, and Yeongsanpo sites are on the main stems of the five major rivers (Han, Nakdong, Geum, Seomjin, and Yeongsan Rivers, respectively) and have the largest basin areas among the chosen sites for each river. Thus, contributions of most parts of the basins to river flows and N exports can be assessed at these sites.

The Yeongdeungpo site is located near the outlet of the Han River, and its basin consists of 16 subbasins, which vary in land use and associated anthropogenic N inputs (Figure 1 and Table 2). The basin includes two major tributaries of the Han River: South Han River (SHR) and North Han River (NHR). The SHR flows along extensive agricultural land and larger residential districts (subbasins 1–7), whereas the NHR flows through mostly forested land, with a few small residential districts (subbasins 9–15). The main stem of the Han River originates at the confluence of the SHR and NHR and flows through the Seoul-Incheon metropolitan area (subbasins 8, 15, and 16), considerably affected by high emissions of oxidized reactive nitrogen (NO_X) from a rapid increase in the number of vehicles (OECD, 2006). We divided these 16 subbasins into six groups by combining one to three subbasins (Figure 1 and Table 2). We attempted for each of the six groups to have similar amounts of N inputs (10.18–11.46 kt/year), yet with varying areal N input rates (2,543–5,497 $kg{\cdot}km^{-2}{\cdot}year^{-1}$; Table 2).

River flow and water-quality data were obtained from Ministry of Land, Infrastructure and Transport and National Institute of Environmental Research. Water-quality data were analyzed for total nitrogen (TN), dissolved nitrogen (DN), dissolved nitrite (NO_2^-) plus nitrate (NO_3^-) nitrogen (DNO_{23}-N), and dissolved ammonium (NH_4^+) nitrogen (DNH_4-N) in milligrams per liter. The data show that the sum of the DNO_{23}-N and DNH_4-N from many sites is higher than DN. Because nitrate is not likely to be adsorbed to soil particles, DNO_{23}-N should not be very different from total nitrite and nitrate nitrogen (TNO_{23}-N). However, if the water samples were not filtered or coarse filters were used, this may have resulted in overestimation of DNH_4-N. Thus, here we only use DNO_{23}-N data for model evaluation and refer to DNO_{23}-N as nitrate N instead of nitrate plus nitrite N since the amount of nitrite is minor compared to that of nitrate N.

2.2. Model Description, Forcing, and Simulations

LM3-TAN (Lee et al., 2014) was developed by integrating coupled terrestrial water, C, and N cycling of Geophysical Fluid Dynamic Laboratory LM3V-N (Gerber et al., 2010; Shevliakova et al., 2009) with a global river routing and lake model (Milly et al., 2014), river N cycling processes and inputs, and new terrestrial N cycling processes, such as soil denitrification and point N sources to rivers (i.e., sewage). The model captures key mechanisms that control the fate of N, with explicit representation of N transformations within land and N transport to the atmosphere and ocean. Specifically, the model simulates (1) water and energy storage within land and exchanges with the atmosphere at a 30-min time step, (2) five plant functional types (PFTs; C3 and C4 grasses, temperate deciduous, tropical, and cold evergreen trees), (3) C and/or N storage within and exchanges between the vegetation-soil-river system, and (4) land use changes for four land use types (primary land [i.e., land undisturbed by human activities during land use reconstruction], secondary land [i.e., abandoned agricultural land or regrowing forest after logging], cropland, and pasture).

LM3-TAN is spatially gridded, and each grid consists of up to 15 tiles (1 primary land, 1 cropland, 1 pasture, 1 lake, 1 glacier, and up to 10 secondary land tiles). Each tile represents unique perturbation histories, such as

deforestation and agricultural development. The PFTs are simulated based on total biomass and prevailing climate conditions (Shevliakova et al., 2009). The vegetation pools (leaves, fine roots, sapwood, heartwood, and labile storage) are updated daily to account for processes, such as vegetation growth and allocation, leaf fall and display, and natural and fire-induced mortality. Each C pool in vegetation and organic soils (fast/slow litter and slow/passive soil) is paired with a respective N pool based on a pool-specific C:N ratio (Gerber et al., 2010). Decomposition of soil organic matter releases ammonium N, which is further transformed into nitrite or nitrate N by nitrification. Simulations of biologically available inorganic N species (i.e., ammonium and nitrite plus nitrate) allow accounting for N limitation on vegetation growth and biological N fixation as well as N feedbacks on soil organic matter decomposition and stabilization. Dissolved organic, ammonium, and nitrate plus nitrite N leach from soils to rivers (Lee et al., 2014). These river N are routed downstream with water flows. Microbial processes (mineralization, nitrification, and denitrification) in rivers are simulated by first-order loss function with respect to N content and with an adjustment for the influence of water temperature.

In this study, LM3-TAN was implemented at 1/8° spatial and 30-min temporal resolution. Following multiple centuries of spin-up to grow vegetation and accumulate N in soils, LULCC were simulated by using a scenario of land use transitions, wood harvesting, and shifting cultivation for the period 1700–2005 (Hurtt et al., 2006). The scenario was historically reconstructed by combining contemporary satellite-based spatial patterns of agriculture with historical agricultural and population data. After 2005, LULCC were assumed to remain the same. Preindustrial CO_2 concentration of 286 ppmv was applied up to 1800 and reported annual CO_2 concentrations from the National Oceanic and Atmospheric Administration Earth System Research Laboratory (NOAA, 2018) were applied from 1801 to 2010. The model was forced by historical climates for the period 1948–2010 (Sheffield et al., 2006), which are observation-based, global near-surface meteorology data, including precipitation, specific humidity, air temperature, surface pressure, wind speed, and shortwave and longwave downward radiation at 1° spatial and 3-hr temporal resolution (Sheffield et al., 2006). The 1948–2010 climates were cycled to perform simulations from 1381 to 1947 and then applied for the simulations from 1948 to 2010. Reported preindustrial atmospheric-N deposition (Dentener & Crutzen, 1994; Green et al., 2004) was applied at a uniform annual rate up to 1950 and reported yearly contemporary N inputs from 1999 to 2010 (National Institute of Environmental Research, 2014) were repetitively applied to perform simulations from 1951 to 2010.

The contemporary N input database (National Institute of Environmental Research, 2014) includes nine yearly N input data sets at 1/8° spatial resolution from 1999 to 2010: three contemporary N sources, from atmospheric deposition, agriculture (i.e., sum of fertilizer, manure, and legume), and sewage, with each of the N sources having three N species (i.e., nitrate, ammonium, organic N). Manure and sewage are produced within the land system. Thus, the amount of added manure and sewage N was deducted from simulated N harvest. For each grid cell, which consists of up to 15 land use tiles, atmospheric-N deposition was applied to all of the land tiles, whereas agricultural N was applied only to the cropland tiles. Sewage N was directly applied to rivers. Each of the N species for the three N sources was applied to the corresponding land and river pools respectively. The model structure and description of N applications are illustrated in Figure 1 of Lee et al. (2014), which is available at https://www.biogeosciences.net/11/5809/2014/bg-11-5809-2014.pdf.

The model was calibrated by comparing LM3-TAN results with empirical estimates at the Yeongdeungpo site (126°96′E, 37°51′N), of which basin covers 96% of the Han River Basin (26,219 km^2). The contemporary N inputs were underestimated because they did not account for some N sources in the basins (e.g., partially treated municipal wastewaters during high precipitation events). Seven parameters from Lee et al. (2014) were adjusted to compensate for the effect of underestimated N inputs on nitrate-N exports and calibrate the model (Table 3). Also, LM3-TAN results at 10 additional sites (Figure 1 and Table 1) were evaluated. For the calibration and evaluation, simulated and reported long-term mean and annual river nitrate-N exports from 1999 to 2010 were compared, the latter of which were based on whether p values of both Pearson's correlation coefficient (r) and Spearman's correlation coefficient (r_s) were less than or equal to 0.1.

2.3. Contemporary N Input Reduction Scenarios

The model was run from 2011 to 2073 by using the 2010 climate (Sheffield et al., 2006) cycled for the next 63 years (i.e., without interannual climate variability) and various contemporary N input reduction scenarios (Table 4). N input rates ($kg{\cdot}m^{-2}{\cdot}year^{-1}$) in 2010 were modified for 2011 and beyond as described in Table 4. For example, scenario 1 reduces the 2010 N input rates in a single step by 15%, 30%, and 45%, which reduces

Table 3
Adjusted Seven Parameters

Parameter	Description	Value	Unit	Reference or rationale
Parameters in the land component equations				
r_{DOM}, $r_{NH_4^+}$, $r_{NO_3^-}$	Calibration factors for DOM, ammonium-N, and nitrate-N	1, 2, 3	unitless	Calibrated to match stream N loads Lee et al. (2014)
k_{LF}, k_{LS}, k_{SS}	Decomposition rates of fast litter/soil and slow soil	18.5, 4.8, 0.2	1/year	Parton et al. (1993), Bolker et al. (1998), Gerber et al. (2010)
Parameters in the river component equations				
$k'_{denitr,\,min}$	Minimum reaction rate constant of river denitrification	0.11/86400	1/s	Alexander et al. (2009)

Note. Seven parameters were adjusted from a previous study (Lee et al., 2014). The calibration factors were introduced by Lee et al. (2014) to compensate for processes that were not accounted for in the model, such as impacts of soil microbes and N storage in lentic systems. DOM = dissolved organic matter.

N inputs (kt/year) by 9%, 25%, and 41%. To account for the effects of historical interannual climate variability, the model was also run from 2011 to 2073 using the 63-year (1948–2010) climates (Sheffield et al., 2006) and the various contemporary N input reduction scenarios described in Table 4.

3. Results and Discussions

3.1. Evaluation of River Flows and Nitrate-N Exports

Overall, using the same parameters throughout the entire drainage network of South Korea, river flows (Figure 2) and nitrate-N exports (Figures 3 and 4) were simulated well by LM3-TAN for the period 1999–2010. Twelve-year mean reported and simulated river flows (−25% to +11%) and nitrate-N exports (−39% to +18%, Figure 3a) at the monitoring sites are in good agreement, except at the last downstream flow (Gurye2, +54%) and nutrient (Gurye, +126%) monitoring sites on the Gum River. In general, higher runoff results in higher river flows and N exports (Lee et al., 2014, 2016). Thus, the overestimated flows at Gurye2 appear to contribute to the higher nitrate-N exports in the river. In each of the five main stem rivers, the nitrate-N exports increase gradually with the downstream direction (Figure 3b), as the drainage area, and hence N loading to the river increase with the downstream direction. Between the five rivers, the reported and simulated nitrate-N exports generally higher in rivers with larger drainage basins (Table 1 and Figure 3a). However, higher nitrate N is exported at the Gwangju2 site than at the Dosan site, which has a 2.3 times larger basin area. This can be explained by the very high contemporary N input rate (5,374 kg·km^{-2}·year^{-1}) and precipitation (1,524 mm/year) in the Gwangju2 site basin, compared to those in the Dosan site basin (2,055 kg·km^{-2}·year^{-1} and 1,209 mm/year).

Interannual flow variability at the monitoring sites agrees well with the reported data (Figure 2; $r = 0.62–0.96$, $p \leq 0.03$; $r_s = 0.61–0.96$, $p \leq 0.04$). Interannual nitrate-N export variability at the Pyeongchanggang3, Dosan,

Table 4
Contemporary N Input Reduction Scenarios

Scenario	N input rates (kg·m^{-2}·year^{-1}) in 2010Modified for 2011 and beyond as follows	Modified N sources	Modified basins
1	15, 30, and 45% (which reduces N inputs (kt/year) by 9%, 25%, and 41%)	All	All
2	30%	Atmospheric deposition	All
3	30%	Agriculture	All
4	0.24%/year, 0.48%/year, and 0.71%/year (15%, 30%, and 45% by 2073)	All	All
5	No modification	All	All
6	30%	Atmospheric deposition	Group a
7	30%	Atmospheric deposition	Group b
8	30%	Atmospheric deposition	Group c
9	30%	Atmospheric deposition	Group d
10	30%	Atmospheric deposition	Group e
11	30%	Atmospheric deposition	Group f

Note. Six grouped subbasins (groups a–f) in the Yeongdeungpo site basin are described in Table 2 and Figure 1.

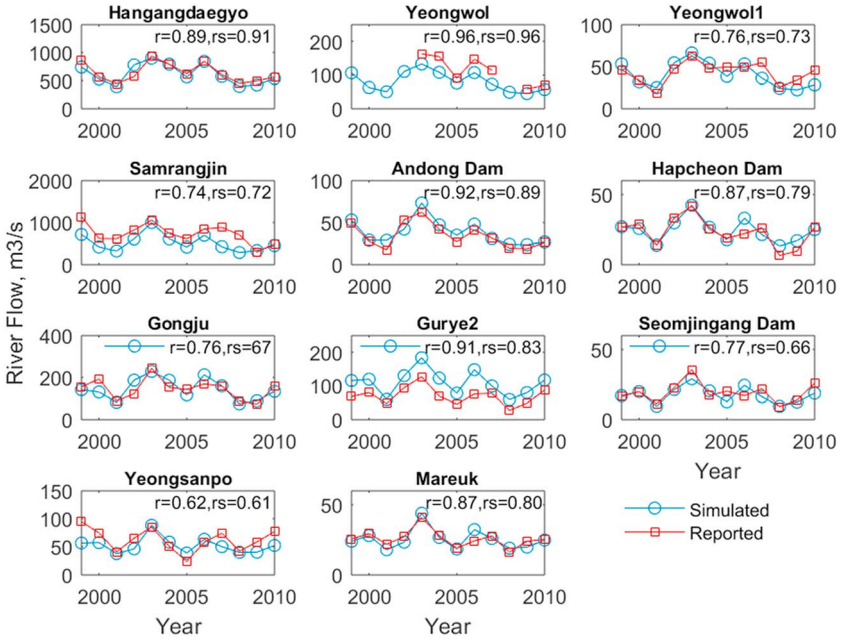

Figure 2. Evaluation of simulated interannual river flows. Temporal patterns of simulated 12-year (1999–2010) annual river flows at the 11 flow monitoring sites, compared with the reported data by using Pearson's correlation coefficients (r) and Spearman's correlation coefficients (r_s).

and Gwangju2 sites (Figure 4; r = 0.57–0.81, $p \leq 0.06$, r_s = 0.58–0.83, $p \leq 0.06$) is also captured well. However, simulated annual nitrate-N exports at the Hwanggang1, Gongju1, Gurye, and Youngsanpo sites are poorly correlated with the reported data (r = 0.19–0.31, r_s = 0.10–0.36). This result may be attributed to unaccounted factors, such as construction in the basins or unresolved processes in the model (e.g., explicit representation of microbes interacting with coupled C and N cycle and vertical distribution of N), as noted in Lee et al. (2014).

3.2. N Storage in Basins

River nitrate-N exports at the 11 sites simulated by cycling the 2010 forcing data (i.e., without interannual climate variability) and using the reduced N inputs by scenarios 1–4 (section 2.3) reach new equilibria (i.e., time points when 12-year mean nitrate-N exports no longer decrease) after 25 to 48 years. For example, nitrate-N exports at the Yeongdeungpo site reach new equilibria after 40 years (Figure 5), indicating the effects of legacy N storage in basins on river N exports under N input reduction efforts. That is, multiple decades may be required to obtain the full effects of N input reductions on river and coastal water quality. We find this result to be consistent with a recent study showing that it takes more than 30 years for Mississippi River nitrate-N exports to reach new equilibria after imposing instantaneous basin-wide reductions in N inputs (Van Meter et al., 2018).

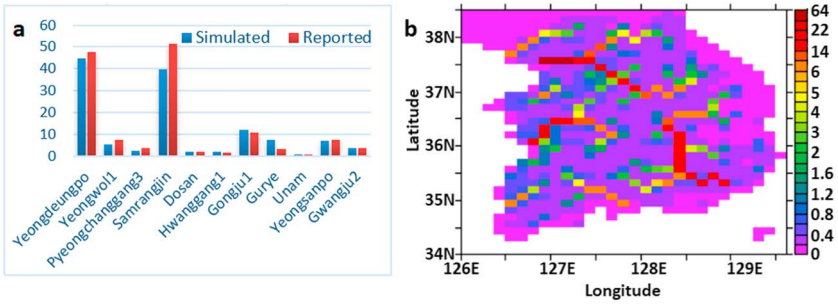

Figure 3. Evaluation of simulated river nitrate-N exports. (a) Simulated and reported river nitrate-N exports (kt/year) in a 7-year (2003–2007 and 2009–2010) average at the Yeongwol1 site, an 11-year (1999–2004 and 2006–2010) average at the Pyeongchanggang3 site, and 12-year (1999–2010) averages at the other nine monitoring sites. (b) Spatial distribution map of simulated 12-year (1999–2010) average stream and river nitrate-N exports (kt/year).

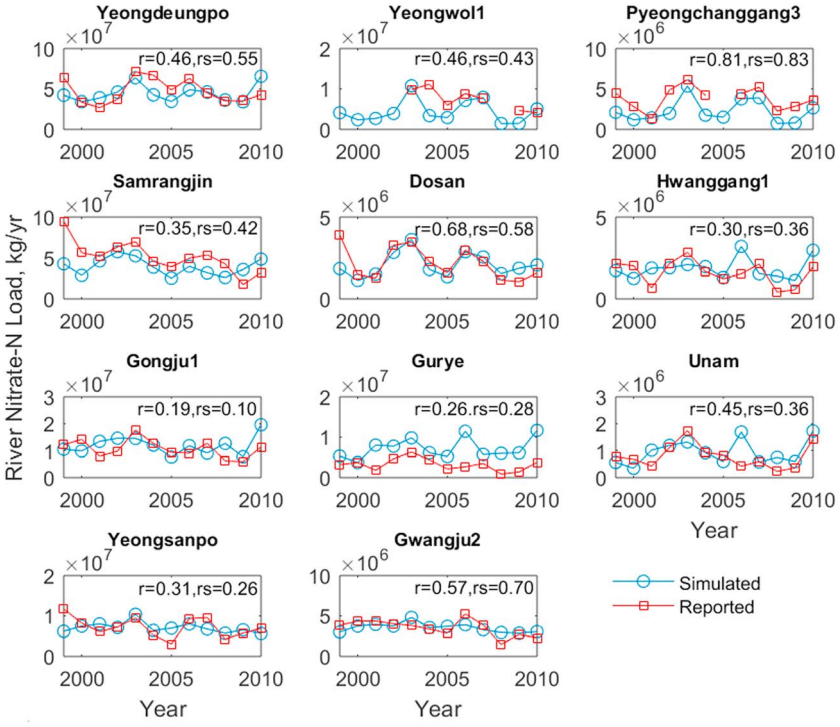

Figure 4. Evaluation of simulated interannual river nitrate-N exports. Temporal patterns of simulated 12-year (1999–2010) annual river nitrate-N exports at the 11 nutrient monitoring sites, compared with the reported data by using Pearson's correlation coefficients (r) and Spearman's correlation coefficients (r_s).

We find that a 9% N input reduction (scenario 1) results in a 41% decrease in river nitrate-N exports at the Yeongdeungpo site (Figure 5). That is, a small reduction in N inputs have a greater improvement on water quality, perhaps because terrestrial and/or aquatic ecosystems in the Han River Basin, including the densely populated, large urban areas, are saturated with respect to N and do not have much capacity to assimilate marginal N inputs under current N loadings. This finding is consistent with a previous empirical study, showing a 33% decrease in Mississippi River nitrate-N exports in response to a 14.2% reduction in net anthropogenic N inputs (defined as the sum of fertilizer, fixation, and atmospheric deposition N inputs minus N exported in food and feed; McIsaac et al., 2001), yet the results differ from a modeling study of the Des Moines River Basin, which reported a 25.2% decrease in nitrate-N exports as a result of a 29.5% reduction in fertilizer (Schilling & Wolter, 2009). However, this discrepancy between our study and McIsaac et al. (2001) versus Schilling and Wolter (2009) is probably because the later only reduced fertilizer N inputs, and other inputs (e.g., atmospheric deposition) were not accounted for when calculating the input reduction percentage.

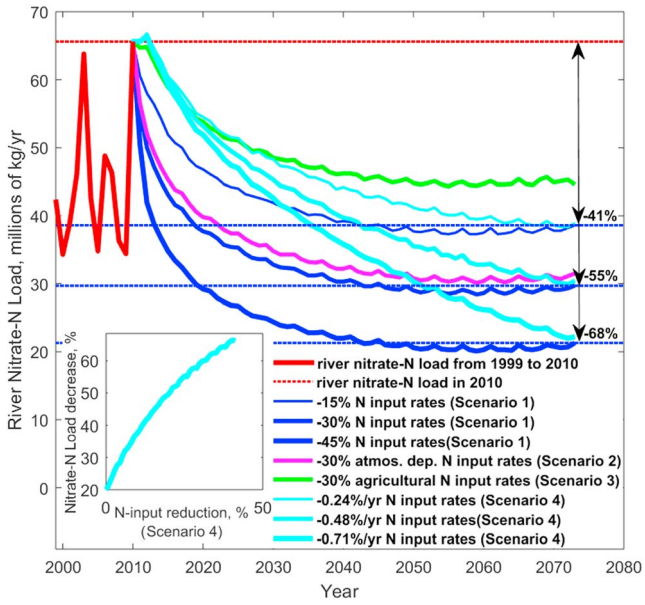

Figure 5. The effect of N storage in basins on river nitrate-N exports. Projected river nitrate-N exports at the Yeongdeungpo site without interannual climate variability under the N input reduction scenarios (scenarios 1–4 in section 2.3).

We also find nonlinear responses of river nitrate-N exports to N input reductions. For example, a 9%, 25%, and 41% N input reduction (scenario 1) results in a 41%, 55%, and 68% reduction in nitrate-N exports at the Yeongdeungpo site (Figure 5). These nonlinear responses, demonstrating decreasing N input reduction efficiency with increasing N input reductions, are further illustrated by a nonlinear relationship between N input reductions (%) by scenario 4 and subsequent nitrate-N export decreases (%; inset in Figure 5). A different response was reported by Chaplot et al. (2004) for the Walnut Creek Basin, where increasing N input reductions of 20%, 40%, and 60% result in 22%, 50%, and 95% decreases in nitrate-N exports. This difference in responses may be a result of different land

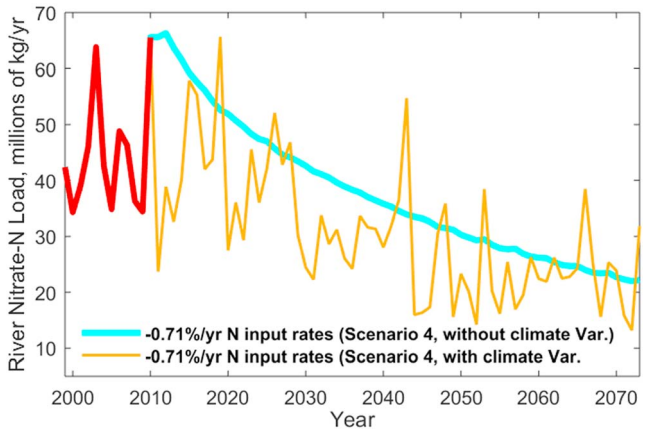

Figure 6. The effect of climate variability on river nitrate-N exports. Projected river nitrate-N loads at the Yeongdeungpo site without and with historical interannual climate variability under the N input reduction scenarios (scenario 4 in section 2.3).

use, levels of N saturation, and precipitation patterns during the growing season between the Han River and Walnut Creek Basins, the latter of 90% is farmed. In such an intensively farmed basin like the Walnut Creek, as N inputs are greatly reduced, N uptake by plants and export via harvesting may enhance N input reduction efficiency.

In the Han River Basin, atmospheric deposition N inputs are much higher than agricultural N inputs. Consistently, comparison between projected nitrate-N exports by using scenario 2 (30% reduction in atmospheric N input rates) and scenario 3 (30% reduction in agricultural N input rates) demonstrates that atmospheric N deposition is the dominant N pollution source in the Han River Basin. This result agrees with an observational study (Chang, 2008), showing that river TN exports at 118 monitoring sites in the Han River Basin had a significant positive relationship with urban land use receiving high atmospheric N deposition yet had a nonsignificant negative relationship with agricultural land use for the period 1993–2002. These results are perhaps, in part, due to a 29% reduction in fertilizer applications from 1997 to 2003 as a result of basin-wide N-reduction efforts, and especially due to the densely populated, large urban areas influenced by intensive NO_X emissions from a number of vehicles (Table 1; OECD, 2006).

3.3. Short-Term Climate Variability and Extremes

Comparison between projected river nitrate-N exports by cycling the 2010 forcing data (i.e., without interannual climate variability) and by using the 63-year forcing data from 1948 to 2010 (i.e., with historical interannual climate variability) demonstrates the effects of climate variability and extremes on nitrate-N exports under N input reductions (scenarios 1–4 in section 2.3). The results show that climate variability can significantly mask the effects of N input reductions on water quality on annual-to-decadal time scales. For example, in Figure 6, nitrate-N exports at the Yeongdeungpo site range from 34 to 66 kt/year in 1999–2010. And then, by the −0.71%/year N input rate reduction (scenario 4), nitrate N exports with climate variability range from 13 to 38 kt/year in 2062–2073, whereas those without climate variability range from 22 to 25 kt/year. Specifically, the highest nitrate N export influenced by climate variability in 2062–2073 is 52% higher than the highest one without climate variability. However, 63-year average nitrate-N export with climate variability (30 kt/year) is lower than the average without climate variability (37 kt/year). These results suggest anthropogenic climate change associated with more frequent and intense extreme weather events (Coumou & Rahmstorf, 2012; Intergovernmental Panel on Climate Change, 2013) may not act to increase river nitrate-N exports averaged over long-term periods yet can significantly mask N input reduction effects by increasing frequency of years with high nitrate-N export extremes associated with recurring coastal hypoxia.

3.4. Long-Term Mean Climate

An analysis of projected river nitrate-N exports at the 11 sites by cycling the 2010 forcing data and using the 45% reduced N input rates (scenario 1) demonstrate the effects of long-term mean climate on river nitrate-N exports under N input reductions. A N input reduction efficiency ratio for each site was calculated as a percentage decrease of mean nitrate-N exports at each site between two periods 1999–2010 and 2062–2073, divided by a percentage decrease of N inputs to each basin between the two periods. For the N conditions in the basins studied here, the efficiency ratios are always greater than 1. A significant negative relationship between the efficiency ratios and basin-wide mean precipitation (Pearson's correlation, $r = -0.82$, $p = 0.002$; Figure 7a) highlights that the effects of N input reductions can be diminished in regions influenced by wetter climate. This result is consistent with an empirical study (Howarth et al., 2006), which showed a greater fractional river N exports of net anthropogenic N inputs in basins influenced by wetter climate. This is perhaps driven by generally shorter water residence times within wetter basins, providing less opportunities for N-removal processes like denitrification in riparian wetlands and low-order streams (Howarth et al., 2006). In contrast, we find no significant relationship between the efficiency ratios and basin-wide mean N input rates ($r = -0.04$, $p = 0.92$). These results imply that long-term mean climate can be a stronger control on geographic variation in N input reduction efficiency than anthropogenic N inputs.

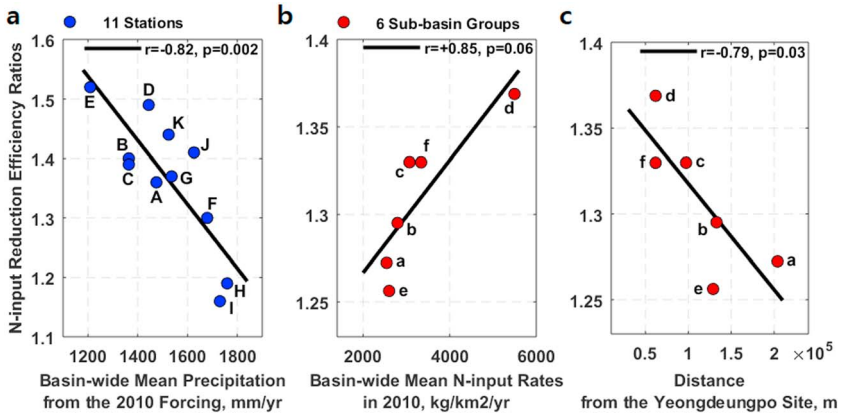

Figure 7. The effects of climate, anthropogenic N inputs, and basin location on river nitrate-N exports. (a) The relationship between basin-wide mean precipitation and N input reduction efficiency ratios for the 11 sites and their basins (Table 1), with Pearson's correlation (*r*) and *p* value (*p*). A N input reduction efficiency ratio was calculated as a percentage decrease of mean nitrate-N exports at each site between two periods 1999–2010 and 2062–2073, divided by a percentage decrease of N inputs to each basin between the two periods. (b and c) The relationships of N input reduction efficiency ratios with (b) six grouped subbasin-wide means of N input rates and (c) distances from the Yeongdeungpo site to the six grouped subbasins (Table 2). A N input reduction efficiency ratio was calculated as a percentage decrease of 2062–2073 mean nitrate-N exports at the Yeongdeungpo site between each of the scenarios 6–11 and the scenario 5 (i.e., no reduction in N input rates), divided by a percentage decrease of 2062–2073 mean N inputs to the Yeongdeungpo site basin between each of the scenarios 6–11 and the scenario 5.

3.5. Anthropogenic N Inputs and Basin Location

The effects of anthropogenic N inputs and basin location on nitrate-N exports under N input reductions are demonstrated by analyzing projected river nitrate-N exports by reducing atmospheric deposition N inputs for each of the six grouped subbasins in the Yeongdeungpo site basin without interannual climate variability (scenarios 6–11). This analysis focused on the one basin, which spans less varying climate conditions, allows minimizing long-term mean climate impacts demonstrated in section 3.4. For these experiments, we chose to reduce only the atmospheric deposition N inputs because it is the dominant N pollution source in the Han River Basin, as demonstrated in section 3.2. A N input reduction efficiency ratio was calculated as a percentage decrease of 2062–2073 mean nitrate-N exports at the Yeongdeungpo site between each of the scenarios 6–11 and the scenario 5 (i.e., no reduction in N input rates), divided by a percentage decrease of 2062–2073 mean N inputs in the Yeongdeungpo site basin between each of the scenarios 6–11 and the scenario 5.

A positive relationship between the efficiency ratios and N input rates ($r = +0.85$, $p = 0.06$; Figure 7b and Table 3) highlights that N exports to the coastal ocean can be reduced more efficiently by decreasing N inputs in subbasins receiving high anthropogenic N inputs. In contrast, a negative relationship of the efficiency ratios with the distances between the six grouped subbasins and the Yeongdeungpo site ($r = -0.79$, $p = 0.03$; Figure 7c and Table 3) indicates that the efficiency of N input reductions increases with shorter water travel time. These two results and implications are consistent with Schilling and Wolter (2009). The higher N input reduction efficiency obtained by targeting subbasins near the basin outlet is also consistent with the facts that (1) shorter travel time provides less opportunities for N-removal processes like river denitrification and (2) N-removal rates in rivers generally decrease with the downstream direction due to increased river channel size or depth (Alexander et al., 2009, 2000). In other words, for subbasins having less opportunities for N-removal processes, direct N input reductions are required to efficiently reduce N exports at the basin outlet. Therefore, the highest N-removal efficiency shown for the *group d* subbasin can be explained by the combined effects of the extremely high N input rate and the close location to the Yeongdeungpo site, which does not allow for much N processing. Whereas the low efficiency shown for the *group e* and *group a* subbasins is because much of the N coming from these sites is processed during the longer travel times; hence, reductions at the sources have lower impacts on N exports at the Yeongdeungpo site.

4. Conclusions

By adjusting only seven parameters from the previous Susquehanna River Basins study (Lee et al., 2014) and using the same parameters for the entire country (100,210 km^2), which encompasses different climate, land use, and geological characteristics, LM3-TAN simulated spatial (11 sites) patterns of long-term (1999–2010) average river flows and nitrate-N exports well, although agreement of interannual variability in nitrate-N exports is limited to several sites (section 3.1). Based on nitrate-N export projections by using multiple scenarios of N input reductions and different climates, this study provides the following fundamental insights for effective basin management strategies to reduce river nitrate-N exports and coastal hypoxia:

- Atmospheric N deposition attributed to high NO_X emissions from vehicles is the dominant N pollution source in the Han River Basin that includes the large urban areas. A small N input reduction in such highly utilized basins can have a greater improvement on water quality, perhaps because their terrestrial and/or aquatic ecosystems do not have much capacity to assimilate added N (section 3.2).
- Heightening climate variability may not increase long-term mean river N exports yet can significantly mask N input reduction effects by producing N export extremes associated with recurring coastal hypoxia (section 3.3).
- Long-term mean climate can be a stronger control on geographic variation in N input reduction efficiency on river nitrate-N exports than anthropogenic N inputs. Although wetter climates likely result in lower N input reduction efficiency (section 3.4), it should be noted that regions influenced by wetter climates generally produce a greater fractional river N exports of net anthropogenic N inputs. Thus, wetter regions with lower N input reduction efficiency may generate much higher river N exports than drier regions with higher N input reduction efficiency, hence targeting wetter basins can be necessary to reduce coastal hypoxia.
- Goals in reducing N sources and monitoring their effects might account for both short-term climate variability and long-term mean climate (sections 3.3 and 3.4).
- Coastal N exports can be most efficiently reduced by decreasing N inputs in subbasins which are receiving high anthropogenic N inputs and are close to the coast (section 3.5).

These implications are driven by river nitrate-N export projections, which are simulated by using the historical 63-year climates or by cycling the same 1-year climate. While this approach allows analyzing possible impacts of various ecosystem factors, including interannual climate variability, on water quality under N input mitigation efforts, results and implications obtained from this approach might be different from those obtained by using future climate scenarios or different historical climate data. For example, unlike our results, future climate change might increase not only high extremes of nitrate-N exports but also their long-term averages if both precipitation averages and variability were to increase. In addition, changing climate forcings will also affect vegetation and soil dynamics, which might have significant impacts on the delivery of terrestrial N to rivers and hence N exports to the coastal environment. Finally, care has to be taken when applying these implications for other basins of which natural or anthropogenic characteristics, such as land use, climates, and basin size, are very different from those in South Korea.

Acknowledgments
We thank P. C. D. Milly from U.S. Geological Survey, C. A. Stock from NOAA/Geophysical Fluid Dynamic Laboratory and two anonymous reviewers for their incisive comments on the manuscript and analyses. Support for M. Lee was provided by a Fulbright Scholarship, by the Princeton Environmental Institute at Princeton University through the Mary and Randall Hack'69 Research Fund, and by the NOAA (U.S. Department of Commerce) grants NA08OAR4320752 and NA14OAR4320106. This study was partially supported by the research project "Impact assessment of climate change on water quality in a regional scale using a land surface model" of the National Institute of Environmental Research. The data used in this study and model outputs are extensively described where needed and attached to this article as supporting information Data Sets S1 and S2. The model codes are available at https://github.com/minjinl/LM3-TAN. Annual CO_2 concentrations from the NOAA Earth System Research Laboratory are available at http://www.esrl.noaa.gov/gmd/ccgg/trends/global.html; last access: 21 January 2018. The authors declare that there are no conflicts of interest regarding the publication of this paper.

References

Alexander, R. B., Böhlke, J. K., Boyer, E. W., David, M. B., Harvey, J. W., Mulholland, P. J., et al. (2009). Dynamic modeling of nitrogen losses in river networks unravels the coupled effects of hydrological and biogeochemical processes. *Biogeochemistry*, *93*(1-2), 91–116. https://doi.org/10.1007/s10533-008-9274-8

Alexander, R. B., Smith, R. A., & Schwarz, G. E. (2000). Effect of stream channel size on the delivery of nitrogen to the Gulf of Mexico. *Nature*, *403*(6771), 758–761. https://doi.org/10.1038/35001562

Bolker, B. M., Pacala, S. W., & Parton, W. J. (1998). Linear analysis of soil decomposition: Insights from the CENTURY model. *Ecological Applications*, *8*, 425–439.

Breitburg, D. (2002). Effects of hypoxia, and the balance between hypoxia and enrichment, on coastal fishes and fisheries. *Estuaries*, *25*(4), 767–781. https://doi.org/10.1007/BF02804904

Chang, H. (2008). Spatial analysis of water quality trends in the Han River basin, South Korea. *Water Research*, *42*, 3285–3304. https://doi.org/10.1016/j.watres.2008.04.006

Chaplot, V., Saleh, A., Jaynes, D. B., & Arnold, J. (2004). Predicting water, sediment and NO3-N loads under scenarios of land-use and management practices in a flat watershed. *Water, Air, and Soil Pollution*, *154*(1-4), 271–293. https://doi.org/10.1023/B:WATE.0000022973.60928.30

Coumou, D., & Rahmstorf, S. (2012). A decade of weather extremes. *Nature Climate Change*, *2*(7), 491–496. https://doi.org/10.1038/nclimate1452

Dentener, F. J., & Crutzen, P. J. (1994). A three-dimensional model of the global ammonia cycle. *Journal of Atmospheric Chemistry*, *19*(4), 331–369. https://doi.org/10.1007/BF00694492

Diaz, R. J., & Rosenberg, R. (1995). Marine benthic hypoxia: A review of its ecological effects and the behavioural responses of benthic macrofaunal. *Oceanography and Marine Biology*, *321*, 926–929.
Diaz, R. J., & Rosenberg, R. (2008). Spreading dead zones and consequences for marine ecosystems. *Science*, *321*(5891), 926–929. https://doi.org/10.1126/science.1156401
Galloway, J. N., Dentener, F. J., Capone, D. G., Boyer, E. W., Howarth, R. W., Seitzinger, S. P., et al. (2004). Nitrogen cycle: Past, present and future. *Biogeochemistry*, *70*(2), 153–226. https://doi.org/10.1007/s10533-004-0370-0
Galloway, J. N., Townsend, A. R., Erisman, J. W., Bekunda, M., Cai, Z., Freney, J. R., et al. (2008). Transformation of the nitrogen cycle: Recent trends, questions, and potential solutions. *Science*, *320*(5878), 889–892. https://doi.org/10.1126/science.1136674
Gerber, S., Hedin, L. O., Oppenheimer, M., Pacala, S. W., & Shevliakova, E. (2010). Nitrogen cycling and feedbacks in a global dynamic land model. *Global Biogeochemical Cycles*, *24*, GB1001. https://doi.org/10.1029/2008GB003336
Green, P. A., Vorosmarty, C. J., Meybeck, M. J., Galloway, N., Peterson, B. J., & Boyer, E. W. (2004). Pre-industrial and contemporary fluxes of nitrogen through rivers: A global assessment based on typology. *Biogeochemistry*, *68*(1), 71–105. https://doi.org/10.1023/B:BIOG.0000025742.82155.92
Hagy, J. D., Boynton, W. R., Keefe, C. W., & Wood, K. V. (2004). Hypoxia in Chesapeake Bay, 1950–2001: Long-term change in relation to nutrient loading and river flow. *Estuaries*, *27*(4), 634–658. https://doi.org/10.1007/BF02907650
Howarth, R. W., & Marino, R. (2006). Nitrogen as the limiting nutrient for eutrophication in coastal marine ecosystems: Evolving views over three decades. *Limnology and Oceanography*, *51*(1part2), 364–376. https://doi.org/10.4319/lo.2006.51.1_part_2.0364
Howarth, R. W., Sharpley, A., & Walker, D. (2002). Sources of nutrient pollution to coastal waters in the United States: Implications for achieving coastal water quality goals. *Estuaries*, *25*(4), 656–676. https://doi.org/10.1007/BF02804898
Howarth, R. W., Swaney, D. P., Boyer, E. W., Marino, R., Jaworski, N., & Goodale, C. (2006). The influence of climate on average nitrogen export from large watersheds in the northeastern United States. *Biogeochemistry*, *79*(1-2), 163–3186. https://doi.org/10.1007/s10533-006-9010-1
Hu, X., McIsaac, G. F., David, M. B., & Louwers, C. A. L. (2007). Modeling riverine nitrate export from an East-Central Illinois Watershed using SWAT. *Journal of Environmental Quality*, *36*(4), 996–1005. https://doi.org/10.2134/jeq2006.0228
Hurtt, G. C., Frolking, S., Fearon, M. G., Moore, B., Shevliakova, E., Malyshev, S., et al. (2006). The underpinnings of land-use history: Three centuries of global gridded land-use transitions, wood-harvest activity, and resulting secondary lands. *Global Change Biology*, *12*(7), 1208–1229. https://doi.org/10.1111/j.1365-2486.2006.01150.x
Hyun, J. H., Choi, J. K., Chung, K. H., Yang, E. J., & Kim, M. K. (1999). Tidally induced changes in bacterial growth and viability in the macro-tidal Han River estuary, Yellow Sea. *Estuarine, Coastal and Shelf Science*, *48*(2), 143–153. https://doi.org/10.1006/ecss.1998.0421
Intergovernmental Panel on Climate Change (2013). In F. Stocker, et al. (Eds.), *Climate change 2013: Detection and attribution of climate change: From global to regional: The physical science basis*. Cambridge, UK: Cambridge University Press.
Jha, M. K., Gassman, P. W., & Arnold, J. G. (2007). Water quality modeling for the Raccoon River Watershed using SWAT. *Transactions of the ASABE*, *50*, 479–493.
Johnes, P. J. (1996). Evaluation and management of the impact of land-use change on the nitrogen and phosphorus load delivered to surface waters: The export coefficient modelling approach. *Journal of Hydrology*, *183*(3-4), 323–349. https://doi.org/10.1016/0022-1694(95)02951-6
Kaushal, S. S., Groffman, P. M., Mayer, P. M., Striz, E., & Gold, A. J. (2008). Effects of stream restoration on denitrification in an urbanizing watershed. *Ecological Applications*, *18*(3), 789–804. https://doi.org/10.1890/07-1159.1
Kemp, W. M., Boynton, W. R., Adolf, J. E., Boesch, D. F., Boicourt, W. C., Brush, G., et al. (2005). Eutrophication of Chesapeake Bay: Historical trends and ecological interactions. *Marine Ecology Progress Series*, *303*, 1–29. https://doi.org/10.3354/meps303001
Krause, S., Jacobs, J., Voss, A., Bronstert, A., & Zehe, E. (2008). Assessing the impact of changes in landuse and management practices on the diffuse pollution and retention of nitrate in a riparian floodplain. *Science of the Total Environment*, *389*(1), 149–164. https://doi.org/10.1016/j.scitotenv.2007.08.057
Lee, M., Malyshev, S., Shevliakova, E., Milly, P. C. D., & Jaffé, P. R. (2014). Capturing interactions between nitrogen and hydrological cycles under historical climate and land use: Susquehanna watershed analysis with the GFDL land model LM3-TAN. *Biogeosciences*, *11*(20), 5809–5826. https://doi.org/10.5194/bg-11-5809-2014
Lee, M., Shevliakova, E., Malyshev, S., Milly, P. C. D., & Jaffé, P. R. (2016). Climate variability and extremes, interacting with nitrogen storage, amplify eutrophication risk. *Geophysical Research Letters*, *43*, 7520–7528. https://doi.org/10.1002/2016GL069254
McIsaac, G. F., David, M. B., Gertner, G. Z. G., & A, D. (2001). Nitrate flux in the Mississippi River. *Nature*, *414*(6860), 166–167. https://doi.org/10.1038/35102672
McLauchlan, K. K., Williams, J. J., Craine, J. M., & Jeffers, E. S. (2013). Changes in global nitrogen cycling during the Holocene epoch. *Nature*, *495*(7441), 352–355. https://doi.org/10.1038/nature11916
Milly, P. C. D., Malyshev, S. L., Shevliakova, E., Dunne, K. A., Findell, K. L., Gleeson, T., et al. (2014). An enhanced model of land water and energy for global hydrologic and Earth-system studies. *Journal of Hydrometeorology*, *15*(5), 1739–1761. https://doi.org/10.1175/JHM-D-13-0162.1
Mulholland, P. J., Helton, A. M., Poole, G. C., Hall, R. O., Hamilton, S. K., Peterson, B. J., et al. (2008). Stream denitrification across biomes and its response to anthropogenic nitrate loading. *Nature*, *452*(7184), 202–205. https://doi.org/10.1038/nature06686
Murphy, R. R., Kemp, W. M., & Ball, W. P. (2011). Long-term trends in Chesapeake Bay seasonal hypoxia, stratification, and nutrient loading. *Estuaries and Coasts*, *34*(6), 1293–1309. https://doi.org/10.1007/s12237-011-9413-7
National Institute of Environmental Research (2014), Studies on impact assessment of climate change on water quality in a regional scale using a Land Surface Model (II), Incheon, South Korea.
NOAA (National Oceanic and Atmospheric Administration) (2018). NOAA Earth System Research Laboratory: available at: www.esrl.noaa.gov/gmd/ccgg/trends (last access: 21 January 2018).
Organisation for Economic Cooperation and Development (OECD) (1997). OECD Environmental Performance Reviews Korea.
Organisation for Economic Cooperation and Development (2006). OECD Environmental Performance Reviews Korea.
Paerl, H. W., Valdes, L. M., Peierls, B. L., Adolf, J. E., & Harding, L. W. Jr. (1998). Ecosystem responses to internal and watershed organic matter loading: Consequences for hypoxia in the eutrophying Neuse River Estuary, North Carolina, USA. *Marine Ecology Progress Series*, *166*, 17–25. https://doi.org/10.3354/meps166017
Parton, W. J., Scurlock, J. M. O., Ojima, D. S., Gilmanov, T. G., Scholens, R. J., Schimesl, D. S., et al. (1993). Observations and modeling of biomass and soil organic matter dynamics for the grassland biome worldwide. *Global Biogeochemical Cycles*, *7*, 785–809.
Peterson, B. J., Wollheim, W. M., Mulholland, P. J., Webster, J. R., Meyer, J. L., Tank, J. L., et al. (2001). Control of nitrogen export from watersheds by headwater streams. *Science*, *292*(5514), 86–90. https://doi.org/10.1126/science.1056874

Rabalais, N. N., Turner, R. E., Justic´, D., Dortch, Q., & Wiseman Jr., W. J. (1999). Characterization of hypoxia: Topic 1 Report for the integrated assessment of hypoxia in the Gulf of Mexico. NOAA Coastal Ocean Program Decision Analysis Series no. 15. NOAA Coastal Ocean Program, Silver Spring, Maryland.

Rabalais, N. N., Turner, R. E., Sen Gupta, B. K., Boesch, D. F., Chapman, P., & Murrell, M. C. (2007). Hypoxia in the northern Gulf of Mexico: Does the science support the plan to reduce, mitigate, and control hypoxia? *Estuaries and Coasts*, *30*(5), 753–772. https://doi.org/10.1007/BF02841332

Rabalais, N. N., Turner, R. E., & Wiseman, W. J. Jr. (2002). Gulf of Mexico hypoxia, A.K.A. "the dead zone". *Annual Review of Ecology and Systematics*, *33*(1), 235–263. https://doi.org/10.1146/annurev.ecolsys.33.010802.150513

Schilling, K. E., & Wolter, C. F. (2009). Modeling nitrate-nitrogen load reduction strategies for the Des Moines River, Iowa Using SWAT. *Environmental Management*, *44*, 671–682.

Sheffield, J., Goteti, G., & Wood, E. F. (2006). Development of a 50-yr high-resolution global dataset of meteorological forcings for land surface modelling. *Journal of Climate*, *19*(13), 3088–3111. https://doi.org/10.1175/JCLI3790.1

Shevliakova, E., Pacala, S. W., Malyshev, S., Hurtt, G. C., Milly, P. C. D., Caspersen, J. P., et al. (2009). Carbon cycling under 300 years of land-use changes: Importance of the secondary vegetation sink. *Global Biogeochemical Cycles*, *23*, GB2022. https://doi.org/10.1029/2007GB003176

Smil, V. (1999). Nitrogen in crop production: An account of global flows. *Global Biogeochemical Cycles*, *13*, 647–662. https://doi.org/10.1029/1999GB900015

Van Meter, K. J., Van Cappellen, P. N., & Basu, B. (2018). Legacy nitrogen may prevent achievement of water quality goals in the Gulf of Mexico. *Science*, *360*(6387), 427–430. https://doi.org/10.1126/science.aar4462

Wendland, F., Bogena, H., Goemann, H., Hake, J. F., Kreins, P., & Kunkel, R. (2005). Impact of nitrogen reduction measures on the nitrogen loads of the river Ems and Rhine (Germany). *Physics Chemistry of the Earth, Parts A/B/C*, *30*(8-10), 527–541. https://doi.org/10.1016/j.pce.2005.07.007